Supported Metal Particles from LDH Nanocomposite Precursors: Control of the Metal Particle Size at Increasing Metal Content

C. Gérardin, D. Kostadinova, N. Sanson, B. Coq, and D. Tichit*

Laboratoire de Matériaux Catalytiques et Catalyse en Chimie Organique, UMR 5618 CNRS-ENSCM-UM1, Institut C. Gerhardt FR 1878, 8 Rue Ecole Normale, 34296 Montpellier Cedex 5, France

Received July 20, 2005. Revised Manuscript Received October 13, 2005

A family of nanocomposites formed by intercalation of negatively charged Ni-based nanoparticles in Mg/Al layered double hydroxide (LDH) has been prepared by following the anion exchange route. The composites differ by the amount of loaded Ni entities. Suspensions of Ni nanoparticles have been priorily prepared by controlled hydroxylation of Ni^{2+} cations in the presence of citrate complexing ions. Intercalated Ni complex colloids exhibit the same behavior in the different composites upon reduction. The nanocomposite route leads after reduction at 1023 K to controlled amounts of metal Ni nanoparticles presenting a similar mean size of 5 nm and a high degree of dispersion on a magnesium/aluminum oxide matrix.

Introduction

There has always been a strong incentive for developing highly selective supported metal catalysts. Their properties can be finely tuned by the use of metal−support interaction and cooperation. Among the acidic supports, various layered materials have been used for the preparation of such catalysts. Nanoparticles exhibiting catalytic, photocatalytic, or semiconducting properties have thus been immobilized in the interlamellar space of clay minerals or in the porous network of pillared clays (PILCs).[1−6] The advantage is that the steric hindrance in the interlayer space prevents aggregation of the nanoparticles and allows the control of their growth. In some cases, the nanoparticle formation has been achieved by reduction of charge-compensating metallic cations giving rise to intercalated metal nanoparticles.[6] An other interesting method has been successfully applied for the introduction of Pd into montmorillonite or PILCs.[1−3] Pd particles have thus been obtained by reduction of palladium acetate in the adsorption layer acting as a "nanophase reactor" on the surface of the clay mineral particles. This adsorption layer formed by a liquid binary mixture of ethanol and toluene is enriched in ethanol at the surface of the clay layer, where reduction is achieved.

Surprisingly, interaction and cooperation between nanosized metal particles and basic supports have been scarcely investigated. A recent review has shown the great potential of layered double hydroxides (LDH) as precursors of metal particles on basic supports with very unique properties,[7,8] as regards metal−support interaction ("electron transfer") and metal−support cooperation ("metal-base bifunctional catalysis"). LDHs of general formula $[M^{2+}_{1-x}M^{3+}_{x}(OH)_2][A^{n-}_{x/n}\cdot m\,H_2O]$ can contain different M^{2+} and M^{3+} metal cations in their brucite-like sheets, and various A^{n-} charge-compensating anions in their interlayer space. LDH compounds easily decompose into mixed oxides of the $M^{II}M^{III}(O)$ type after calcination.[9−11] Three general routes are available for obtaining, from LDHs precursors, materials having both basic and redox functions: First, the synthesis of LDHs containing M^{II} and/or M^{III} elements with redox behavior within the sheets; second, the exchange with anionic metal precursors of the desired metal in the interlayer space of the LDHs; third, the deposition or grafting of inorganic or organometallic precursors onto the calcined precursor LDH. However these routes of catalysts preparation suffer from several limitations: (i) pure LDH phases cannot be obtained with a noble metal content larger than 5 at. %;[12,13] (ii) catalytically active ions of too large ionic radius or without octahedral coordination cannot be accommodated in the brucite-like sheets;[9,14] and (iii) the sizes of the metal particles obtained after calcination and reduction of the LDH or mixed oxides are not easily controlled, aggregation often takes place leading to large particle sizes.[15−18] Keeping in mind these drawbacks, there

* To whom correspondence should be addressed. Fax: +33 (0)467163470. E-mail: didier.tichit@enscm.fr.

(1) Szücs, A.; Király, Z.; Berger, G.; Dékány, I. *Colloids Surf. A* **1998**, *139*, 109.
(2) Szücs, A.; Berger, G.; Dékány, I. *Colloids Surf. A* **2000**, *174*, 387.
(3) Dékány, I.; Turi, L.; Király, Z *Appl. Clay Sc*i. **1999**, *15*, 221.
(4) Németh, J.; Dékány, I; Süvegh, K.; Marek, T.; Klencsár, Z.; Vértes, A.; Fendler, J. H. *Langmuir* **2003**, *19*, 3762.
(5) Mogyorósi, K.; Dékány, I; Fendler, J. H. *Langmuir* **2003**, *19*, 2938.
(6) Patakfalvi, R; Oszkó, Dékány, I. *Colloids Surf. A* **2003**, *220*, 45.
(7) Vaccari, A.; *Appl. Clay Sci*. **1999**, *14*, 161.
(8) Tichit, D.; Coq, B. *Cattech* **2003**, *7*, 206.
(9) Cavani, F.; Trifirò, F.; Vaccari, A *Catal. Today* **1991**, *11*, 173.
(10) De Roy, A.; Forano, C.; El Malki, K.; Besse, J. P. In *Synthesis of Microporous Materials*; Occelli, M. L., Robson, H., Eds.; Van Nostrand Reinhold: New York, 1992.
(11) Rives, V. *Layered Double Hydroxides*: *Present and Future*; Nova Science Publishers: New York, 2001.
(12) Basile, F.; Basini, L.; Fornasari, G.; Gazzano, M.; Trifirò, F.; Vaccari, A. *J. Chem. Soc., Chem. Commun.* **1996**, 2435.
(13) Basile, F.; Fornasari, G.; Gazzano, M.; Vaccari, A. *Appl. Clay Sci.* **2000**, *16*, 185.
(14) Vaccari, A. *Catal. Today* **1998**, *41*, 53.
(15) Titulaer, M. K.; Ben, J.; Jansen, H.; Geus, J. W. *Clays Clay Miner*. **1994**, *42*, 249.
(16) Marquevich, M.; Farriol, X.; Medina, F.; Montané, D. *Catal. Lett*. **2003**, *85*, 41.

10.1021/cm051588h CCC: $30.25
Published on Web 11/16/2005

is a demand to design new synthesis routes for obtaining highly loaded metal catalysts with control of metal particles in size and distribution starting from LDH precursors.

A recent report has described a novel preparation method of such materials by intercalation of preformed negatively charged Ni-based nanoparticles in Mg/Al LDH.[19] The colloidal polynuclear precursors are composed of partially hydroxylated Ni cations stabilized by strong complexing agents. In these preliminary reports, it was shown that a better control of nanosized Ni^0 particles can be achieved. Three approaches can be considered in order to prepare LDHs nanocomposites incorporating large negatively charged entities: the LDH coprecipitation and the reconstruction (based on the so-called "memory affect") of the host LDH in the presence of the anionic species, and the anion exchange route of, for example, nitrate-containing LDH with the anions.[19−21] Regarding anionic large polynuclear Ni colloids, the two former methods yield poorly ordered layer structures;[19] in contrast, the exchange method yields well-ordered lamellar structures. Moreover, the anionic exchange route is the only one that allows us to tailor Ni particle sizes in the calcined and reduced materials.

It is worthy to note some recent attempts to incorporate metal complexes in a way similar to that described above. Efficient catalysts of methane reforming were thus obtained using Mg/Al-LDH intercalated with $[Ni(Edta)]^{2-}$ (Edta: ethylenediaminetetraacetate) species as precursors.[22] As an alternative way, the organic chelating agent Edta was first intercalated by anion exchange into the LDH host and the desired metal ion in solution was then complexed by reaction with the Edta-Li/Al LDH. The chelation process between the ligand Edta and the transition metal ions (Co, Ni, Cu) was extensively studied.[23] However, this material elaboration method did not successfully achieve a control of the metal particle size.

The aim of the present work was therefore the tailoring of the Ni content in the LDH nanocomposites and the fine control in size and distribution of the Ni metal particles after reduction. For this purpose original Ni-containing LDH nanocomposites were prepared by exchanging various amounts of preformed negatively charged Ni colloids with controlled sizes.

Experimental Section

Preparation of Ni Colloids. Colloidal suspensions of Ni-based particles were obtained by hydrolysis of an aqueous solution of $Ni(NO_3)_2 \cdot 6H_2O$ (0.5 M) and $Na_3(C_6O_7H_3)$ with NaOH (O.5 M). The molar ratio [citrate]/[Ni] was 1. Hydrolysis of Ni^{2+} ions was performed at a controlled nickel hydroxylation ratio [OH]/[Ni] = 1.

Preparation of HDL Host Structures and Nanocomposites. The host NO_3-Mg/Al sample (Mg/Al = 2) was prepared by coprecipitation at constant pH (≈10) of suitable amounts of $Mg(NO_3)_2 \cdot 6H_2O$ (0.2 M), $Al(NO_3)_3 \cdot 6H_2O$ (0.1 M) with a solution of NaOH (1.0 M). Addition of the alkaline solution was controlled by using a pH-STAT Titrino (Metrohm) apparatus to keep the pH constant. The suspension was stirred overnight at 353 K for 17 h, and then the solid was separated by centrifugation, washed thoroughly with distilled water (Na < 100 ppm), and dried overnight at 353 K. These samples will be hereafter labeled NO_3-Mg/Al LDH.

The Ni_x-Mg/Al nanocomposites of variable Ni contents were prepared from the NO_3-Mg/Al LDH by anionic exchange of nitrate ions; 3 g of the host Mg/Al LDH was dispersed in the required amounts of a 0.03 M aqueous suspension of Ni-based nanoparticles ([citrate]/[Ni] = 1; [OH]/[Ni] = 1) corresponding to $x = 0.35$, 0.7, 1, and 1.4 times the theoretical anionic exchange capacity (AEC estimated to 4.8 mequiv g^{-1}) in Mg/Al LDH. For this purpose the solids were dispersed in 300, 250, 166, and 83 cm^3 of solution, respectively. The exchange process was performed by stirring the mixture in air at room temperature for 12 h. The solid was then recovered and washed by dispersion and centrifugation in deionized water and finally dried at 353 K for 12 h. These samples were hereafter labeled $Ni_{0.35}-Mg/Al$ LDH for example for the nanocomposite obtained by intercalation of Mg/Al LDH with an amount of Ni colloidal suspension theoretically corresponding to 0.35 times the AEC.

Characterization. Chemical analyses of both as-prepared samples and calcined materials at 723 K were performed at the Service Central d'Analyse du CNRS (Solaize, France).

Hydrodynamic sizes of the nickel hydroxide colloids were determined by dynamic light scattering at 90° using a 4800 Malvern Autosizer. XRD patterns were recorded on a Bruker D8 Advance instrument using the Cu $K\alpha_1$ radiation ($\lambda = 1.542$ Å, 40 kV, and 50 mA).

N_2 sorption experiments at 77 K were carried out on samples previously calcined at 723 K and outgassed at 523 K (10^{-4} Pa) with a Micromeritics ASAP2000 instrument. Specific surface areas were calculated using the BET method.

TG-DSC experiments were carried out using a Setaram TG-DSC-111 apparatus, with fully programmable heating and cooling sequences, sweep gas valve switchings, and data analysis. The sample were placed in a platinum crucible and dried at 393 K under He stream (flow: 20 cm^3 min^{-1}). Heating was then performed at 5 K min^{-1} from room temperature up to 1073 K in a stream of He or synthetic air (flow: 20 cm^3 min^{-1}). A Balzers QMS 421 quadrupole mass spectrometer equipped with a SEM detector (0−200 amu) was used to conduct analysis of the evolved gases during parallel experiments of TG-DSC, under the same conditions of activation, nature of gases and heating ramp.

The H_2 temperature-programmed reduction (TPR) analyses were done using a Micromeritics AutoChem 2910 instrument with a TCD detection ($m = 30$ mg, H_2/Ar: 25/75, flow = 30 cm^3 min^{-1}, ramp = 10 °C/min). The H_2 consumption was determined after trapping H_2O at ca. 200 K.

TEM analysis of samples was performed using a JEOL 1200 EXII microscope operated at 80 kV on samples previously calcined at 723 K and then reduced at 873 K. Measurements of the reduced nickel particle sizes on several micrographs led to the determination of the mean particle sizes

Results and Discussion

A colloidal suspension of nickel hydroxy citrate entities was prepared. A first step of Ni^{2+} ions complexation by

(17) Morioka, H.; Shimizu, Y.; Sukenobu, M.; Ito, Tanabe, K.; Shishido, T.; Takehira, K. *Appl. Catal. A* **2001**, *215*, 11.
(18) Olafsen, A.; Slagtern, Å.; Dahl, I. M.; Olsbye, U.; Schuurman, Y.; Mirodatos, C. *J. Catal.* **2005**, *229*, 163.
(19) Gerardin, C.; Kostadinova, D.; Sanson, N.; Francova, D.; Tanchoux, N.; Tichit, D.; Coq, B. *Stud. Surf. Sci. Catal.* **2005**, *156*, 357.
(20) Khan, A. I.; O'Hare, D. *J. Mater. Chem.* **2002**, *12*, 3191.
(21) Rives, V.; Ulibarri, M. A. *Coord. Chem. Rev.* **1999**, *181*, 61
(22) Tsyganok, A. I.; Suzuki, K.; Hamakawa, S.; Takehira, K.; Hayakawa, T. *Catal. Lett.* **2001**, *77*, 75.
(23) Tarasov, K. A.; O'Hare, D.; Isupov, V. P. *Inorg. Chem.* **2003**, *42*, 1919.

Table 1. Composition Obtained from Chemical Analysis and Proposed Formula, BET Surface Area, and H_2/Ni Molar Consumption Ratio of the Ni-LDH Nanocomposites

sample	chemical composition wt % Mg	Al	Ni	N	C	formula	SS[a] ($m^2\ g^{-1}$)	H_2/Ni[b]
Mg/Al	18.20	10.3		4.14	0.40	$[Mg_{0.66}Al_{0.34}(OH)_2][(CO_3)_{0.04}(NO_3)_{0.26}]\cdot 0.5H_2O$		
$Ni_{0.35}$−Mg/Al	16.02	9.37	3.75	1.28	5.77	$[Mg_{0.66}Al_{0.34}(OH)_2][(NO_3)_{0.09}(CO_3)_{0.052}[Ni(C_6O_7H_3)_{1.12}(OH)]_{0.063}]\cdot mH_2O$	270	1.21
$Ni_{0.7}$−Mg/Al	14.59	8.34	6.64		9.14	$[Mg_{0.66}Al_{0.34}(OH)_2][(CO_3)_{0.03}[Ni(C_6O_7H_3)_{1.085}(OH)]_{0.123}]\cdot mH_2O$	320	1.34
Ni_1−Mg/Al	14.47	8.24	7.32		9.07	$[Mg_{0.66}Al_{0.34}(OH)_2][(CO_3)_{0.024}[Ni(C_6O_7H_3)_{1.05}(OH)]_{0.136}]\cdot mH_2O$	280	1.32
$Ni_{1.4}$−Mg/Al	14.30	8.14	7.32		9.26	$[Mg_{0.66}Al_{0.34}(OH)_2][(CO_3)_{0.031}[Ni(C_6O_7H_3)_1(OH)]_{0.138}]\cdot 0.55H_2O$	300	1.22 (0.9)[c]

[a] BET specific surface area determined on samples calcined at 723 K and outgassed at 523 K. [b] From TPR experiments of the samples pretreated at 723 K under N_2. [c] From TPR experiments of the samples pretreated at 773 K under air.

citrate complexing agents in solution leads to the formation of a solution of Ni complexes with a pH of 5.6. It was followed by hydrolysis of the complexed Ni ions using sodium hydroxide: the OH/Ni ratio of 1 leads to a suspension that is transparent and presents a pH of 9.8. That pH value is compatible with the stability of LDH phases and with the further step of intercalation by anionic exchange. The hydrodynamic diameter of the hydrolyzed species formed is about 1.5 nm, and the clusters are negatively charged due to the electrostatic stabilization brought by the citrate ions. These entities then present the right characteristics to be intercalated between LDH layers. Intercalation of Ni entities in varying proportions leads to a series of Ni LDH nanocomposites.

The elemental analyses of the samples reported in Table 1 allow the calculation of the structural formulas of the materials. The Mg/Al molar ratio in the nanocomposites is the same as in the host Mg/Al LDH. The carbon content obtained from elemental analyses is too high to be due only to citrate entities. If we assume that all carbon is in the form of citrates and charge is equilibrated in the nanocomposites, the composition found for the Ni-containing complexes will lead to Ni complexation degrees (citrate/Ni) and hydrolysis degrees (OH/Ni) higher than the expected value of 1 in the theoretical formulas $[Ni(C_6O_7H_3)(OH)]^{2-}$. This suggests that the carbon content in the samples accounts for the presence of both citrate anions as guest entities and carbonate anions in the interlayer space of the host LDH. Following this hypothesis, an estimation of the amounts of carbon involved in citrate and carbonate can be obtained assuming a charge balance between the Al^{3+} cations in the brucite like layers and the anions in the interlayer space, and assuming that the hydrolysis degree in the intercalated complexes equals the theoretical value (OH/Ni = 1). This leads to the Ni-nanocomposites formulas proposed in Table 1. The intercalated Ni-containing complexes exhibit compositions close to the theoretical ones. The amounts of Ni complexes retained by the host LDH are in agreement with those in solution when the Ni content increases up to the AEC value (Figure 1). Above the AEC value, the excess Ni colloids are not accommodated by the composite structure, and they remain as expected in solution. The contamination with carbonates during exchange reactions in air limits the amount of intercalated Ni complexes to about 80% of the AEC. It is noteworthy that in the intercalation of Li/Al LDH with $[NiCl_4]^{2-}$ ions, the exchange rate reaches only 90% despite four successive exchanges with amounts of ions in solution corresponding to 2.5 times the AEC of the LDH. This was

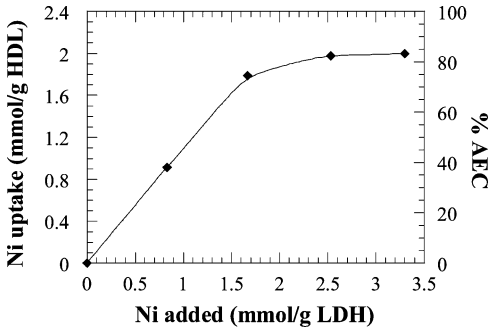

Figure 1. Ni uptake (mmol/g) and % of the AEC of the host Mg/Al LDH as a function of the amount of Ni in solution.

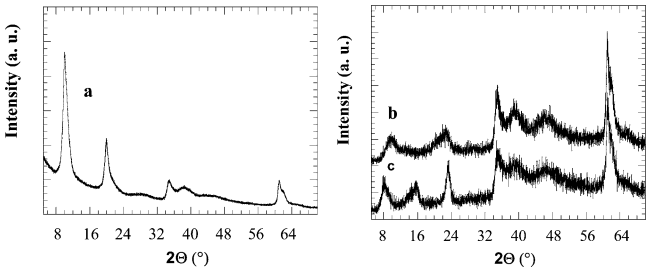

Figure 2. XRD patterns of (a) NO_3−Mg/Al, (b) $Ni_{0.35}$−Mg/Al, and (c) $Ni_{1.4}$−Mg/Al samples.

attributed to the co-existence of carbonates.[24] From the chemical analyses, it was calculated that the Ni content in the present LDHs nanocomposites varies between 3.8 and 7.3 wt %.

The powder XRD patterns of the host LDH, and of the Ni nanoparticles-exchanged LDHs are shown in Figure 2. In all cases the XRD patterns are typical of LDHs structures. The reflections can be indexed in a hexagonal lattice with a $R\bar{3}$m rhomboedral symmetry. The two sharp and intense characteristic diffraction lines appearing as symmetric lines at 2Θ angles below 25° in the Mg/Al LDH are ascribed to (003) and (006) planes. The basal spacing value of d_{003} = 0.880 nm is consistent with the presence of nitrates as charge compensating anions in the interlayer space. This basal spacing corresponds to a lattice ***c*** parameter of 0.264 nm ($\boldsymbol{c} = 3 \times d_{003}$). Wide and asymmetric reflections are observed at higher 2Θ values. The (110) reflection of the LDH structure allows to calculate the ***a*** lattice parameter of 0.304 nm ($\boldsymbol{a} = 2 \times d_{110}$). This value is in agreement with a Mg/Al molar ratio of 2 in the brucite-like layer.[9]

Compared to the XRD pattern of the host LDH, those of the Ni colloids-exchanged LDHs show several changes. Crystallinities greatly decrease indicating a lower ordering

(24) Okada, K.; Matsushita, F.; Hayashi, S. *Clay Miner*. **1997**, *32*, 299.

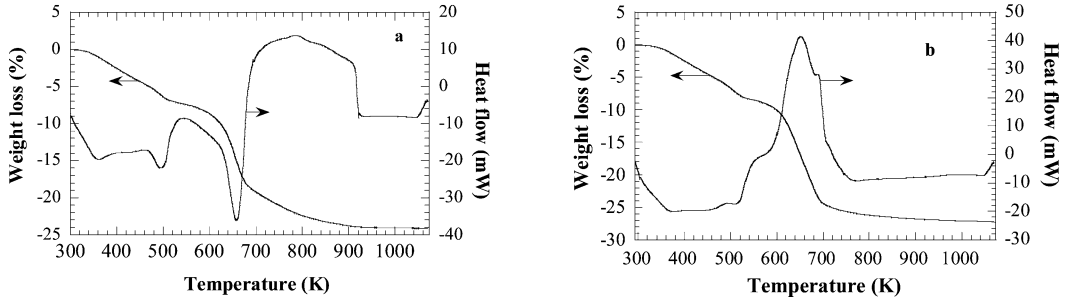

Figure 3. TG-DSC profiles of $Ni_{1.4}$−Mg/Al performed under (a) helium flow and (b) air flow.

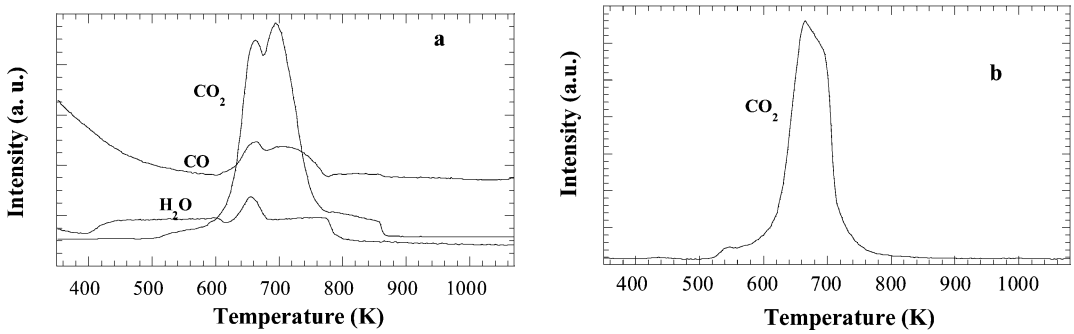

Figure 4. Analysis of the gases evolved during thermal decomposition of of $Ni_{1.4}$−Mg/Al followed by mass spectrometry under (a) He flow and (b) air flow.

in the structural arrangement. Excepted in the case of $Ni_{0.35}$−Mg/Al, three reflections orders (003), (006), and (009) are observed in the 2Θ range below 30°. A displacement toward lower 2Θ values of the (003) diffraction lines in comparison with the host Mg/Al sample denotes an increase of the basal spacing to 1.090 nm. This confirms the intercalation of the anionic clusters within the LDH layers. The thickness of the intercalated colloid species can be calculated by substracting the thickness of the brucite-like layers (estimated to be 0.480 nm) to the d_{003} spacing; the obtained value is about 0.610 nm. It is worthy to note that this value of the thickness is smaller than that corresponding to citrate anions (0.720 nm) intercalated with a vertical orientation within Mg/Al LDH of the same charge density (Mg/Al = 2).[25] Therefore, citrate ions in the Ni complexes must exhibit a conformation different from that observed when they are the only compensating anions. A remarkable feature is the unexpected high intensity of the line at 2Θ 23.20°. This results from the overlapping of the (009) diffraction line due to the Ni colloids and of the (006) diffraction line due to carbonates. Reversed intensities of lines (006) and (009) have been previously reported for LDH intercalated with drugs[26] or polyoxometalate anions[27] and attributed to different planar electron densities.

Only two broad and weak reflections are observed in the case of $Ni_{0.35}$−Mg/Al LDH in the 2Θ range below 30°. Moreover the reflection at 22.68° could not be the (006) higher order of the (003) reflection at 10.04° according to the general relation among the (00*l*) lines ($d_{003} = 2 \times d_{006}$). The first broad line extending from 2Θ 8 to 13° results from the overlapping of the two (003) diffraction lines characteristic of the presence of nitrate anions and Ni colloids. They indeed represent 44 and 30 mol % of the intercalated species, respectively. The second diffraction line shows a maximum at 2Θ 23.20° accounting for the (009) line due to the Ni colloids and a net shoulder toward low 2Θ values assignable to the (006) line of the nitrate anions.

Thermal decomposition of $Ni_{1.4}$−Mg/Al (Ni-rich sample) has been studied by TG-DSC analysis in helium and air flow coupled with mass spectrometry (MS) in order to monitor the nature of the gases released (heating rate: 5 K min^{-1}). We followed in particular masses corresponding to O_2 (16), H_2O (17, 18), CO (28), and CO_2 (44, 28), which take into account the products of decomposition of the intercalated species. As it can be seen in Figure 3a, three regions of mass losses under He are observed, corresponding to endothermic peaks in the DSC profile. The first weight loss, taking place between room temperature and 523 K, appears as a continuous step. It corresponds to a broad peak of H_2O release and accounts for the desorption of physisorbed and interlayer water molecules (Figure 4a). Two separated endotherms are clearly identified as it was also observed in the case of Mg/Al LDH containing glyphosate anions;[28] the endotherms were assigned to the presence of interlayer water molecules confined in a smaller region due to grafting of the anions. It suggests in the present study that water molecules could also be confined between Ni-containing complexes in the nanocomposites. The second weight loss takes place between 523 and 673 K. It is associated to an endothermic peak with H_2O, CO, and CO_2 release. This corresponds to the partial dehydroxylation of the brucite-like layers and decomposition of carbonates as well as citrate species of the intercalated Ni complexes. A third step in the TG plot occurs between

(25) Tronto, J.; Dos Reis, M. J.; Silvério, F.; Balbo, V. R.; Marchetti, J. M.; Valim, J. B. *J. Phys. Chem. Solids* **2004**, *65*, 475.
(26) Del Arco, M.; Cebadera, E.; Gutiérrez, S.; Martin, C.; Montero, M. J.; Rives, V.; Rocha, J.; Sevilla, M. A. *J. Pharm. Sci*. **2004**, *93*, 1649.
(27) Kwon, T.; Pinnavaia, T. J. *Chem. Mater.* **1989**, *1*, 381.
(28) Li, F.; Zhang, L.; Evans, D. G.; Forano, C.; Duan, X. *Thermochim. Acta* **2004**, *424*, 15.

673 and 1073 K. It gives a broad endothermic event and corresponds to the second part of the splitted and intense peak of CO_2 release; H_2O evolution concurrently occurs. These features suggest that in this temperature range, decomposition of entrapped citrate species and dehydroxylation of the layers take place.

As expected, the TG-DSC analysis carried out in oxidative atmosphere provides different results (Figure 3b); this is particularly true above 500 K. The most remarkable feature is the intense exothermic peak extending from 500 to 773 K. It can be attributed to the combustion of the citrate species as it corresponds to intense CO_2 release and O_2 consumption (Figure 4b). In the same temperature range, the TG profile shows 2 steps of weight losses as also observed in inert atmosphere. However, two main differences are observed; the first step goes till 703 K, instead of 673 K in inert atmosphere, and leads to a higher weight loss (29% instead of 24%). It is worthy to note in the MS profiles that hardly no CO_2 evolution occurs above 703 K in air, whereas the CO_2 release is intense and extends till 823 K in helium. Decomposition of citrate species by combustion under oxidative atmosphere is therefore achieved 100 K lower than in inert atmosphere. Accordingly, when comparing weight losses above 723 K under inert and oxidative atmospheres, they represent 8.5% and 3.9% of the total weight, respectively. In the latter case, it corresponds only to the final step of dehydroxylation of the LDH. Therefore the citrate amount remaining at 723 K in the former sample, pretreated under inert atmosphere, could be estimated to 4.6%. This represents about 20% of the initial citrate content. Total weight losses at 1073 K (50.5%) are very close to the value of 52.7% expected for decomposition of $Ni_{1.4}$−Mg/Al into the corresponding oxides.

Specific surface areas of the nanocomposites thermally treated at 723 K in air range between 270 and 320 $m^2\ g^{-1}$, which is significantly higher than that of the calcined host Mg/Al sample (192 $m^2\ g^{-1}$). This probably accounts for both a craterisation phenomenon due to the decomposition of the citrate anions[9] and the obtention of a mixture of different metal oxide phases.

Reduction of the different Ni-containing nanocomposites has been studied from TPR experiments (heating rate: 5 K min^{-1}) on the samples pretreated in inert atmosphere (nitrogen) at 723 K. The XRD patterns of these heat treated samples show the presence of a poorly crystallized mixed oxide phase of the MgO type (Figure 2). This is in agreement with the results of TG analysis showing a high extent of dehydroxylation and decomposition of the intercalated species at 723 K. The different TPR profiles of heated Ni_x-Mg/Al samples exhibit similar shapes whatever the Ni content. There are two domains of H_2 uptake (Figure 5). The first intense peak abruptly rises with a maximum rate of H_2 consumption at 743 K, while the second broad peak exhibits a maximum at ca. 940 K. In all cases reduction is completed at 1053 K. Accordingly, XRD patterns recorded on the reduced samples after TPR experiments at 1273 K, show the presence of a Ni phase and a spinel phase very similar to $MgAl_2O_4$. The total H_2 uptake corresponds to H_2/Ni ratios in the range of 1.2−1.3 (Table 1); these ratios are higher

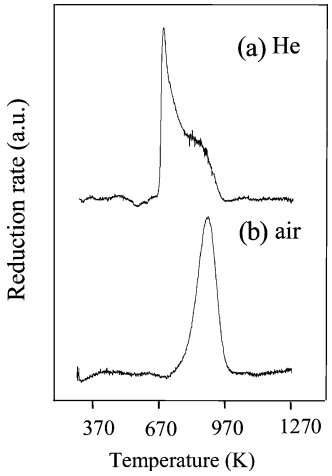

Figure 5. TPR profiles of Ni(1.4) −Mg/Al pretreated (a) at 723 K under helium and (b) at 773 K under air.

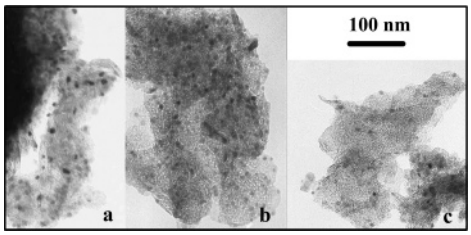

Figure 6. TEM images after treatment at 723 K of (a) $Ni_{1.4}$−Mg/Al under air flow, (b) $Ni_{1.4}$−Mg/Al under N_2 flow, and (c) $Ni_{0.35}$−Mg/Al under N_2 flow and then reduced at 873 K.

than that required for the stoechiometric reduction of Ni^{2+} into Ni (H_2/Ni = 1). However, it was concluded from the previous TG-DSC analysis of $Ni_{1.4}$−Mg/Al that nearly 20% of the initial citrate content were not yet decomposed after heat treatment at 723 K in inert atmosphere. We can postulate that hydrogenation of the remaining organic species during the TPR experiment gives rise to the intense peak of H_2 consumption at 743 K. This was checked by performing a TPR experiment on the $Ni_{1.4}$−Mg/Al sample pretreated at 773 K in air. The TPR profile of the air-calcined sample exhibits only one peak with a maximum at 990 K (Figure 5); the intense peak at lower temperature previously observed after activation at 723 K in nitrogen was absent. Moreover, the H_2 consumption of the sample heat-treated in air corresponds to a molar ratio H_2/Ni = 0.93 in close agreement with the expected value of 1.

It is worth noting that the maximum rate of H_2 consumption for the reduction of Ni^{2+} into Ni^0 occurs at about 940 K, whatever the Ni content of the nanocomposites. This behavior is in contrast with that previously reported for the reduction of NiMg(Al)O oxides obtained from multicomponent coprecipitated Ni/Mg/Al LDH, for which reducibility of Ni becomes easier at higher Ni content.[29] This shows that a rather different reduction process takes place, probably due to the different environments of Ni ions in the precursors: brucite-like layers and citrate-containing complexes.

The final reduced materials were characterized by TEM in order to compare the size distribution of metal particles at various Ni contents. First, the influence of the atmosphere

(29) Tichit, D.; Medina, F.; Coq, B.; Dutartre, R. *Appl. Catal. A* **1997**, *159*, 241.

of heat treatment, prior to reduction, was investigated. TEM images were taken of $Ni_{1.4}$−Mg/Al previously treated in air and in nitrogen and then reduced by H_2 up to 873 K. Figure 6 shows that the mean particle size in sample $Ni_{1.4}$−Mg/Al (air 723 K) equals about 6.5 nm and particles sizes span from 2 to 11 nm, while the average size is about 4.5 nm in $Ni_{1.4}$−Mg/Al (N_2 723 K) and sizes vary from 2 to 7 nm. It appears that heat treatment in N_2 of Ni LDH nanocomposite precursors leads after reduction to smaller Ni particles with a narrower size distribution than that obtained with air calcination. The difference observed here must certainly be due to the different decomposition processes of the organic moieties: first, decomposition of citrates is completed at higher temperature in N_2 than under air flow; second, the energetics is different: the high exothermicity of citrate calcination in air may favor Ni ions diffusion and Ni segregation. These observations, obtained on the sample issued from the total NO_3^- exchange for Ni clusters in the composite precursor, prompted us to treat the whole series of Ni_x-Mg/Al precursors by heating under nitrogen. Figure 6 also allows us to compare TEM images of samples of different Ni content. $Ni_{0.35}$−Mg/Al and $Ni_{1.4}$−Mg/Al both heat treated under N_2 flow at 723 K and reduced with H_2 at 873 K exhibit Ni particles of very similar sizes: the distribution is centered around 5 nm, and the population is rather monodisperse. It is also clearly observed that metal particles are more numerous in samples of higher Ni content. An important result is then the success in maintaining the particle size small and constant when increasing the Ni content. That result could not be achieved with Ni/Mg/Al LDH prepared from the conventional synthesis route by coprecipitation, for which larger Ni^0 particles resulted from increasing Ni contents. Again, the control of the metal dispersion state at increasing metal content may be due to the energetics (thermogravimetry and calorimetry profiles) of organics decomposition. As long as the Ni complexing functions are not completely decomposed, Ni ions must be confined in a carbon-rich protecting shell, which inhibits their diffusion and segregation. It may then not be surprising to observe small particles for a metal content varying from 8 to 15 wt %.

Conclusions

It was shown that intercalation by anion exchange of preformed Ni colloids of controlled charge and size in the interlayer space of Mg/Al LDH resulted in the formation of Ni colloid−Mg/Al nanocomposites. The anion exchange method used for their preparation allows to carefully control the Ni loading in the nanocomposite. Intercalated nickel hydroxy citrate colloids possess the same composition as that of the nanoparticles in solution and are always accompanied by carbonate anions. Indeed exchange performed in contact with air does not allow to introduce an amount of guest entities corresponding to the AEC of the host LDH. The Ni colloid/LDH nanocomposites are poorly crystallized, but the organization degree increases with the amount of Ni colloid intercalated. TG-DSC studies coupled with mass spectrometry put into evidence the exothermic decomposition process of the organic species, which takes place under oxidizing atmosphere and which is completed 100 K lower than the corresponding endothermic decomposition under inert atmosphere. Reduction at 873 K with hydrogen leads to small Ni particles supported on a Mg(Al)O mixed oxide matrix; the Ni particles have the same mean size of 5 nm at loadings varying between 8 and 15 wt %. Total reduction of Ni is achieved at 1073 K. The metal particles size is slightly smaller when heat treatment is performed under inert atmosphere, and the particle size distribution is also narrower. Sintering of the particles during reduction is probably inhibited by the presence of carbon-rich coating formed by the decomposition of the Ni complexing agents. This leads to solids exhibiting higher metal dispersion than solids obtained from coprecipitated Ni/Mg/Al LDH calcined and reduced at similar temperatures. These Ni supported materials offer interesting outlooks for catalytic or magnetic applications.

CM051588H